Title

Inactivation of mouse Twisted gastrulation reveals its role in promoting Bmp4 activity during forebrain development

Author

De Robertis, Edward M.

Publication Date

2004

DOI

10.1242/dev.00946

Peer reviewed

Inactivation of mouse Twisted gastrulation reveals its role in promoting Bmp4 activity during forebrain development

Lise Zakin and E. M. De Robertis*

Howard Hughes Medical Institute and Department of Biological Chemistry, University of California, Los Angeles, CA 90095-1662, USA

*Author for correspondence (e-mail: derobert@hhmi.ucla.edu)

Accepted 13 October 2003

Development 131, 413-424
Published by The Company of Biologists 2004
doi:10.1242/dev.00946

Summary

Twisted gastrulation (Tsg) is a secreted protein that regulates Bmp signaling in the extracellular space through its direct interaction with Bmp/Dpp and Chordin (Chd)/Short gastrulation (Sog). The ternary complex of Tsg/Chd/Bmp is cleaved by the metalloprotease Tolloid (Tld)/Xolloid (Xld). Studies in *Drosophila*, *Xenopus* and zebrafish suggest that Tsg can act both as an anti-Bmp and as a pro-Bmp. We have analyzed *Tsg* loss-of-function in the mouse. *Tsg* homozygous mutants are viable but of smaller size and display mild vertebral abnormalities and osteoporosis. We provide evidence that *Tsg* interacts genetically with *Bmp4*. When only one copy of *Bmp4* is present, a requirement of *Tsg* for embryonic development is revealed. *Tsg*$^{-/-}$;*Bmp4*$^{+/-}$ compound mutants die at birth and display holoprosencephaly, first branchial arch and eye defects. The results show that Tsg functions to promote Bmp4 signaling during mouse head development.

Key words: Twisted gastrulation, Bmp, Tgfβ, Chordin, Tolloid, Crossveinless, Holoprosencephaly, Vertebral column

Introduction

Growth factors of the bone morphogenetic protein (Bmp) superfamily are major regulators of cell-cell signaling in animal development (Hogan, 1996; Massague and Chen, 2000). A gradient of Bmp activity establishes dorsoventral patterning in both vertebrate and invertebrate embryos. Studies in vertebrates and *Drosophila* have shown that Bmp/Dpp activity is regulated in the extracellular space by a network of secreted proteins including Short gastrulation (Sog)/chordin (Chd), Tolloid (Tld)/Xolloid (Xld) and Twisted gastrulation (Tsg) (De Robertis et al., 2000). The *Drosophila Tsg* mutation was isolated during classical genetic screens for embryonic cuticle defects due to its lack of the amnioserosa, the dorsal-most tissue of the fruit fly embryo (Wieschaus et al., 1984). The *Drosophila Tsg* product is necessary for peak Dpp/Bmp activity in the early *Drosophila* embryo, which is required to form the amnioserosa (Mason et al., 1994). Tsg contains two conserved cysteine-rich domains and was shown to bind both Bmp and Chd (Oelgeschläger et al., 2000). The Tsg N-terminal domain binds to Bmp and shares similarity with the cysteine-rich (CR) Bmp-binding modules of Chd, whereas the C-terminal domain is conserved only among the Tsg homologues (Oelgeschläger et al., 2000; Vilmos et al., 2001; Oelgeschläger et al., 2003a). In addition, *Drosophila Tsg* is highly diffusible and can act at a long distance from its site of expression (Mason et al., 1997).

Tsg has multiple biochemical activities. First, it promotes the formation of stable ternary Bmp/Chd/Tsg complexes (Oelgeschläger et al., 2000; Chang et al., 2001; Larrain et al., 2001; Scott et al., 2001). As this ternary complex prevents binding of Bmp to its cell surface receptors, in this aspect of its function Tsg behaves as a Bmp antagonist. Second, the stability of these inhibitory ternary complexes is controlled by the Tld metalloprotease, which cleaves Chd/Sog at specific sites (Marques et al., 1997; Piccolo et al., 1997). In the presence of Tsg, Chd/Sog is a better substrate for cleavage by the Tld enzyme (Larrain et al., 2001; Scott et al., 2001; Shimmi and O'Connor, 2003). By promoting Chd degradation in the presence of Tld, Tsg releases Bmp that is now able to signal through Bmp receptors. In this second aspect of its activity, Tsg functions to increase Bmp activity (Piccolo et al., 1997; Larrain et al., 2001; Shimmi and O'Connor, 2003).

The opposing functions of the Tsg protein may explain why conflicting results have been reported in various microinjection assays. In *Xenopus*, overexpression of *Tsg* mRNA results in Bmp-promoting effects (Oelgeschläger et al., 2000; Oelgeschläger et al., 2003a; Oelgeschläger et al., 2003b). The opposite observation was made in zebrafish embryos, in which microinjection of zebrafish *Tsg* or *Xenopus Tsg* caused dorsalization (Ross et al., 2001; Oelgeschläger et al., 2003b). These different outcomes have been attributed to the different levels of the Tld protease in the two model embryos (Larrain et al., 2001). In zebrafish, endogenous levels of the Tolloid protease are low, as indicated by the weak phenotype of *tolloid/mini-fin* mutant embryos which are viable and lack the ventral tail fin (Connors et al., 1999). At these low Xolloid concentrations, microinjection of *Tsg* mRNA favors the formation of inhibitory Bmp/Chd/Tsg complexes. In the *Xenopus* embryo, high levels of Tld activity are present, Tsg promotes the cleavage of Chd, and ventralization is observed. However, when the endogenous Tld protease is inhibited by co-injection of dominant-negative *Xld* mRNA the opposite result, dorsalization, is seen (Larrain et al., 2001). These experiments suggest that the proteolytic cleavage of Chd

constitutes the crucial molecular switch between the anti-Bmp and Bmp-promoting activities of Tsg.

Additional evidence on the dual activity of Tsg was provided by the study of point mutations that dissociate Bmp binding and Chd interaction (Oelgeschläger et al., 2003a). Mutations in the N-terminal domain of *Tsg* abolish Bmp binding. Surprisingly, these mutant Tsgs still have potent Bmp-promoting effects in both *Xenopus* and zebrafish embryos (Oelgeschläger et al., 2003a). There is evidence that Tsg might interact with anti-Bmp proteins other than Chd. When *Chd* is mutated in zebrafish *chordino*, overexpression of *Tsg* can further ventralize the embryo (Oelgeschläger et al., 2003a). In *Xenopus*, embryos microinjected with antisense *Chd* morpholino oligos together with *Xenopus Tsg* mRNA display very severe ventralization (Oelgeschläger et al., 2003b). These experiments indicate that some of the activities of Tsg are independent of Chd. A large number of extracellular proteins contain Bmp-binding CR modules of the type present in Chd (Larrain et al., 2000; Abreu et al., 2002; Coffinier et al., 2002), and some of them interact with Tsg (C. Coffinier and E.M.D.R., unpublished). Thus, it appears likely that Tsg interacts with other proteins in addition to Chd and Bmps.

Although multiple activities and interactions of Tsg have been identified in vivo and in vitro, many questions remain unanswered concerning its physiological functions. In particular, whether Tsg is a pro-Bmp (Oelgeschläger et al., 2000; Oelgeschläger et al., 2003a; Oelgeschläger et al., 2003b) or is a Bmp antagonist (Chang et al., 2001; Ross et al., 2001; Scott et al., 2001; Blitz et al., 2003) in a loss-of-function situation in mammals. We report the targeted inactivation of the murine *Tsg* gene. *Tsg* mutant mice were viable and of small size, and presented skeletal defects in the vertebral column. We analyzed the interactions between the *Tsg* and *Bmp4* genes. *Tsg*$^{-/-}$;*Bmp4*$^{+/-}$ compound mutants died at birth and displayed severe holoprosencephaly, eye and first branchial arch defects. As Tsg is required for Bmp4 to function during forebrain formation in a dose-dependent manner, we conclude that Tsg acts to promote Bmp4 signaling during mouse head development.

Materials and methods

Generation of *Tsg* mutant mice

The 5′ (1.5 kb) and 3′ (7 kb) genomic fragments used as recombination arms were isolated from a 129/SVJ mouse BAC library (Incyte Genomics) and subcloned into the pGN vector (Le Mouellic et al., 1990). The construct was electroporated into 129/SVJ ES cells, which were then selected with G418. Homologous recombination was detected by PCR using the following primers: GKOWT (5′ATTGTTTTGAGGGGATTTATTTTGA3′) and GKO (5′CGTGCATCTGCCAGTTTGAG3′). The primers produced a band of 1720 bp. ES cell clone genotypes were verified by Southern blot as indicated in Fig. 1. Mice carrying the *Tsg* mutation were backcrossed into the hybrid strain B6SJl/F1 (Jackson Laboratories). *Bmp4* mutant mice (*Bmp4*^{tm1} allele) were a generous gift from Dr Brigid Hogan (Duke University). They were genotyped by PCR as described (Winnier et al., 1995) and maintained into the hybrid strain B6SJL/F1.

Genotyping and RT-PCR

Tsg mutant mice were genotyped by PCR using the following primers: Tsg22 (5′AGCCTGAATGTTTGAATGTTTA3′), Tsg23 (5′CTTGAATCCTTACCTGAATGAG3′) and LacZ3 (5′TCTGCCAGTTTGAGGGGACGAC3′) as described (Bachiller et al., 2000). Genotyping of embryos after in situ hybridization and photography was performed using the boiling DNA preparation method. For RT-PCR, the primers were Tsg-up (5′GTTCGCGGGAGCTGCTTG3′), Tsg-down: (5′CGACGACGATGTTCCAGTTCAG3′), HPRT forward (5′CACAGGACTAGAACACCTGC3′) and HPRT reverse (5′GCTGGTGAAAAGGACCTCT3′). Tsg-up and Tsg-down are located in the 5′UTR and exon 3 respectively, and yielded a 441 bp band. The HPRT primers produced a 249 bp band.

In situ hybridization, histology and skeletal preparations

In situ hybridization on whole-mount or on cryostat sections was performed as previously described (Henrique et al., 1995). The probes used were: *Bmp4* (Winnier et al., 1995), *Dlx5* (Acampora et al., 1999), *Fgf8* (Crossley and Martin, 1995), *Hex* (Bedford et al., 1993), *Shh* (McMahon et al., 1998) and *Cer1* (Belo et al., 1997). The *Tsg* probe was synthesized using the full-length cDNA cloned in pGEMTeasy, linearized with *Xho*I and transcribed with SP6 RNA polymerase. Newborns and E12.5 to E15.5 embryos were fixed in Bouin's solution, dehydrated, cleared and embedded in paraffin wax. Serial 7 μm sections were stained using Hematoxylin and Eosin or Mallory's Tetrachrome method (Bachiller et al., 2003). Alcian Blue and Alizarin Red skeletal staining (Belo et al., 1998), and Alcian Blue staining at E14.5 (Jegalian and De Robertis, 1992) was as described. β-Gal staining of whole embryos was performed by fixing the embryos in 0.2% glutaraldehyde in PBS for 2 to 15 minutes and staining at 37°C in 1 mg/ml Xgal, 2 mM $MgCl_2$, 0.1 M phosphate buffer pH 7.4, 5 mM potassium ferrocyanide, 5 mM potassium ferricyanide.

Results

Disruption of the *Tsg* locus

Targeted inactivation of the *Tsg* gene was performed by in-frame insertion of the *lacZ* reporter gene into the first exon of *Tsg* at the initiator methionine. This also resulted in the deletion of the first *Tsg* exon, which encodes the initial 40 amino acids of *Tsg* including the entire signal peptide (Fig. 1A). This mutation also caused the loss of stable wild-type *Tsg* transcripts when monitored by RT-PCR of mutant E13.5 embryonic cells (Fig. 1D). We conclude that the *Tsg* mutation represents a complete loss-of-function as it lacks the signal peptide and wild-type *Tsg* mRNA is not expressed.

Comparison of the expression of the *Tsg* mRNA and β-galactosidase (β-gal) activity in E6.5 to E8.5 embryos showed that the *lacZ* reporter gene was expressed at the same time and place as the endogenous *Tsg* gene (Fig. 1, compare E,E′-H,H′). *Tsg* expression was observed at E6.5 in the anterior visceral endoderm and forming primitive streak (Fig. 1E,E′). As gastrulation continued and mesodermal wings formed, *Tsg* expression was observed in the entire mesodermal layer (Fig. 1F,F′,G,G′). At early headfold stage *Tsg* was expressed in head mesenchyme, gut endoderm and ventral neuroectoderm (Fig. 1I). At E8.5, *Tsg* was expressed in ventral neuroectoderm such as basal diencephalon (Fig. 1J), the endoderm of the gut, the posterior eye vesicle and the forming pharyngeal arches (Fig. 1H,H′). We conclude that the in-frame reporter gene faithfully recapitulates the endogenous *Tsg* expression pattern.

Tsg$^{-/-}$ mice are viable and have skeletal defects

To address the function of *Tsg* in vivo, heterozygous animals were mated and their progeny analyzed. Viable homozygous mutants were recovered in Mendelian proportions (e.g., in F1 crosses, of 106 neonates 25 were +/+, 57 were +/– and 24 were

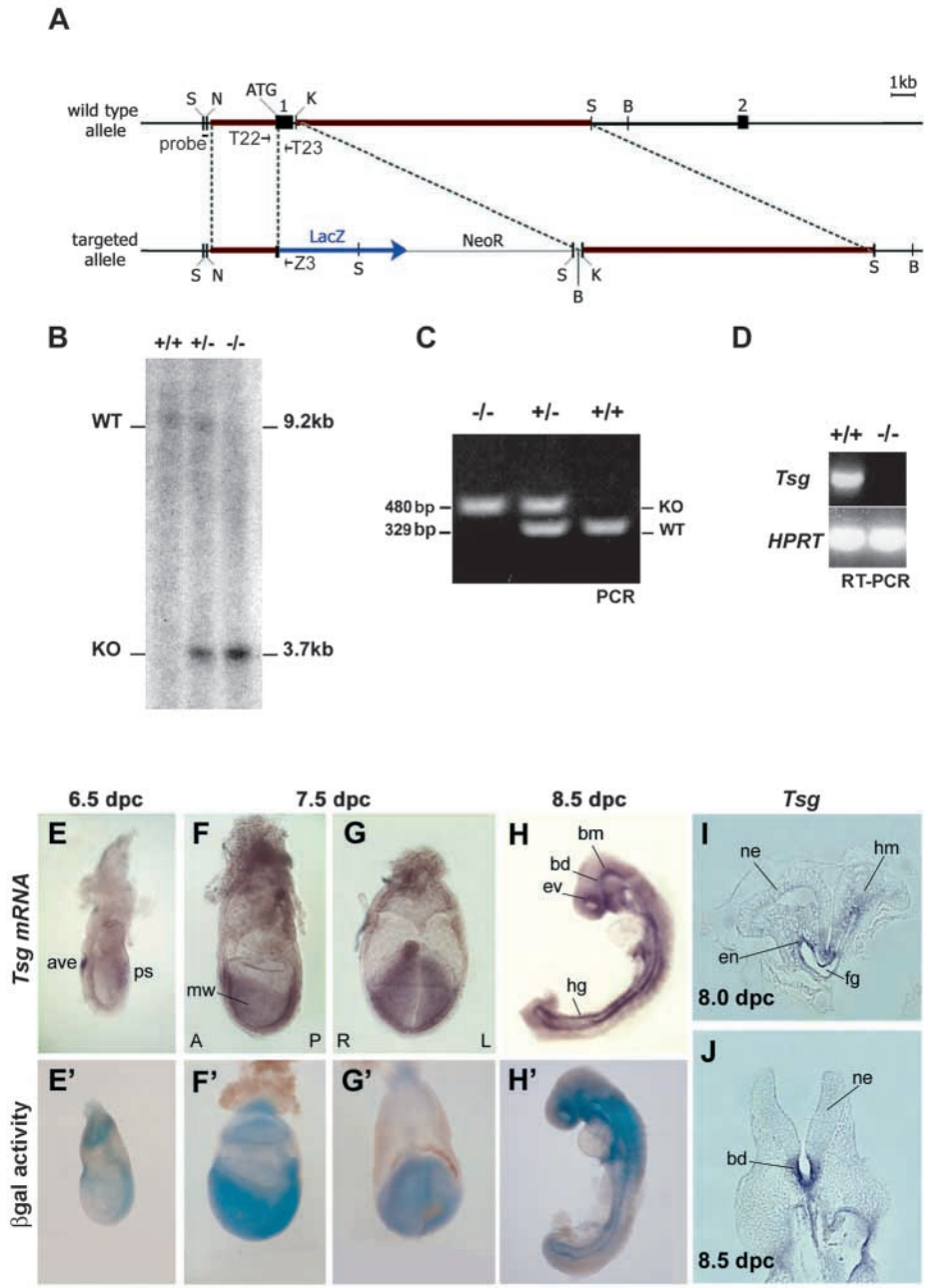

Fig. 1. Genomic organization and expression of the *Tsg* gene. (A) Schematic representation of the wild-type and targeted alleles of *Tsg*. The 5′ probe used for the Southern blot is indicated (probe). The oligonucleotides used for PCR genotyping are shown as arrows: Tsg22, Tsg23 and *lacZ3*. The position of the exons is indicated by black boxes and the recombination arms shown in red. The following restriction sites are indicated: B, *Bam*HI; K, *Kpn*I; N, *Nsi*I; S, *Sac*I. (B) Southern blot analysis of the 5′ genomic region of the *Tsg* gene. DNAs extracted from wild-type, heterozygous and homozygous *Tsg* mutant animals were digested with *Sac*I. The 170 bp *Sac*I-*Nsi*I probe fragment detected a wild-type band of 9.2 kb and a knock out (KO) band of 3.7 kb. (C) PCR genotyping of mice carrying the *Tsg* mutation. The wild-type band of 329 bp was obtained using the Tsg22 and Tsg23 primers. The KO band of 480 bp was obtained using the Tsg22 and *lacZ3* primers. (D) RT-PCR analysis of RNAs extracted from E13.5 wild-type and $Tsg^{-/-}$ embryos showing the absence of *Tsg* mRNA in $Tsg^{-/-}$ embryos. *HPRT* expression was used as a control. (E-H,E′-H′) Comparison of the expression pattern of *Tsg* by whole-mount in situ hybridization and β-galactosidase staining. (E) *Tsg* is expressed in the anterior visceral endoderm and the primitive streak. (F,G) As gastrulation proceeds, *Tsg* is found in the mesodermal layer. (H) At E8.5 *Tsg* is present in the endoderm of the gut, the ventral neural tube and the dorsal region of the eye vesicle. (E′-H′) The expression of the *lacZ* transgene recapitulates the expression of endogenous *Tsg*. (I) Transverse section through the anterior region of an E8.0 embryo showing *Tsg* mRNA in the endoderm of the foregut, ventral neuroectoderm and the head mesenchyme. (J) Section of an E8.5 embryo showing the expression of *Tsg* mRNA in the basal diencephalon. ave, anterior visceral endoderm; bd, basal diencephalon; bm, basal mesencephalon; ev, eye vesicle; en, endoderm; fg, foregut; hg, hindgut; hm, head mesenchyme; mw, mesodermal wings; ne, neuroectoderm; ps, primitive streak; A, anterior; L, left; P, posterior; R, right.

–/–). Both male and female $Tsg^{-/-}$ animals were fertile. Growth analysis of *Tsg* mutants showed that they were of smaller size, weighed 10-20% less than littermates and displayed a short tail. Eighty percent of the $Tsg^{-/-}$ animals presented multiple kinks in the tail, which became more marked with age (Fig. 2A,B). X-rays of adult mice indicated that the caudal vertebrae of mutant mice were shorter than normal and had lower bone density than wild-type or heterozygous animals (Fig. 2B). In E14.5 $Tsg^{-/-}$ embryos, defective cartilage formation was observed in the dorsal neural arches of most cervical and some thoracic vertebrae (Fig. 2C,C′). This defect persisted after birth and was characterized by the incomplete growth and fusion (dyssymphysis) of the osseous vertebral neural arches (compare Fig. 2D with 2D′).

Alcian Blue/Alizarin Red staining revealed the origin of $Tsg^{-/-}$ tail kinks. At birth, $Tsg^{-/-}$ tail vertebrae contained two symmetric centers of ossification, rather than the single axial center observed in wild-type or heterozygous embryos (Fig. 2E,E′). Two weeks later, if the two centers of ossification had grown at the same rate, they produced straight, but shorter vertebrae with vertebral bodies that adopted a bow tie shape (Fig. 2F,F′). In other $Tsg^{-/-}$ vertebrae, the two centers grew asymmetrically, producing hemi-vertebrae that led to misalignment of the articular surfaces and therefore to tail

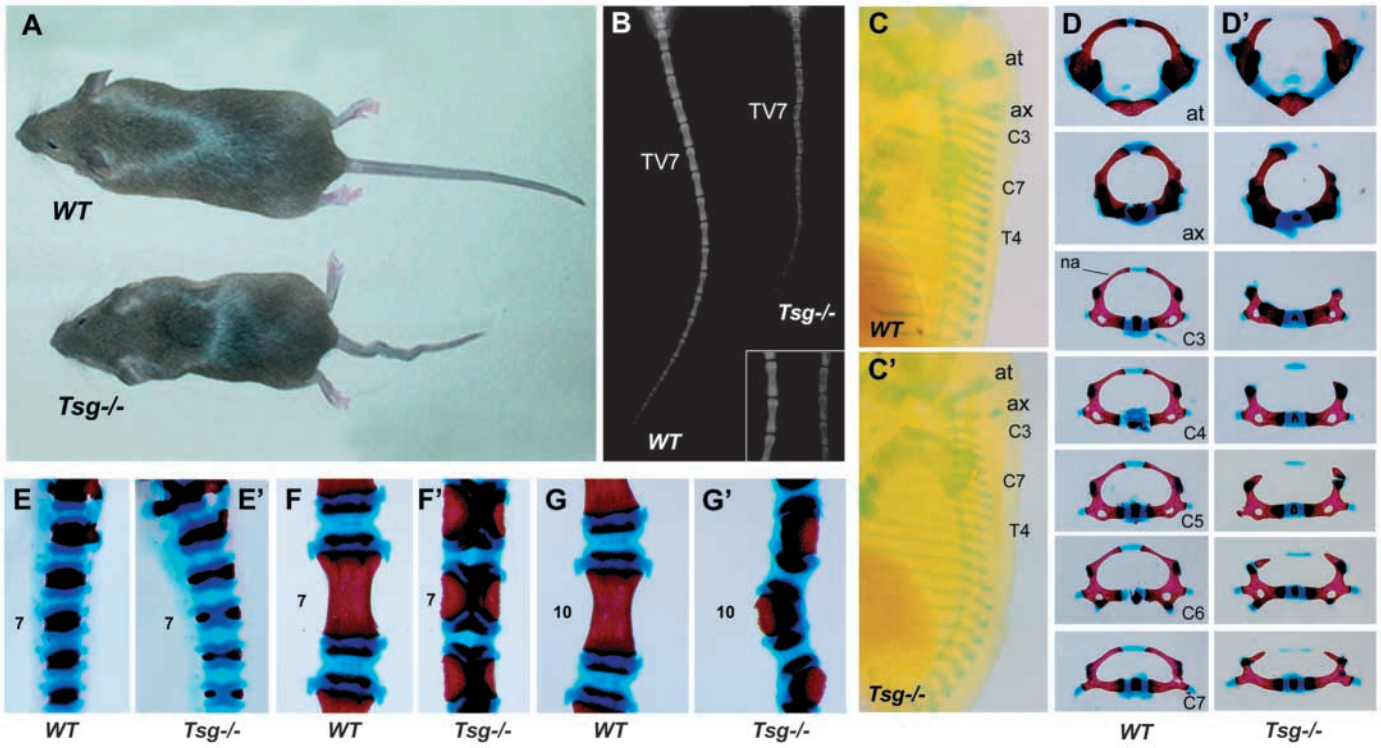

Fig. 2. Skeletal abnormalities in *Tsg*$^{-/-}$ mice. (A) Comparison of 5-week-old wild-type and *Tsg*$^{-/-}$ mice. The *Tsg*$^{-/-}$ mouse is small and displays a short tail with multiple kinks. (B) X-ray of the caudal region of wild-type and *Tsg*$^{-/-}$ adult mice. The tail vertebrae in the mutant are shorter (compare tail vertebra 7, TV7) and have less X-ray opacity (inset). (C-C′) Alcian Blue preparations of E14.5 wild-type and *Tsg*$^{-/-}$ embryos in lateral view. Note the defects in cervical and thoracic neural arch cartilages in *Tsg*$^{-/-}$ embryos. (D-D′) Alcian Blue/Alizarin Red preparations of cervical vertebrae of 2-week old wild-type and *Tsg*$^{-/-}$ mice. The cervical neural arches are not fused dorsally in the mutant. (E-E′) Alcian Blue/Alizarin Red preparations of the caudal regions of wild-type and *Tsg*$^{-/-}$ newborn mice. Note the presence of two centers of ossification in the mutant rather than a single one in the wild-type. The seventh tail vertebra is indicated. (F,F′,G,G′) Skeletal elements of the tail of 2-week old wild-type and *Tsg*$^{-/-}$ mice stained with Alcian Blue/Alizarin Red. (F′) Abnormal vertebrae present a bow-tie shape and are shorter than the wild-type (compare TV7). (G′) One ossification center has failed to form, producing hemi-vertebrae with misaligned articular surfaces, which cause the kinks. at, atlas; ax, axis; C3-7, cervical vertebrae 3-7; na, neural arch; T4, thoracic vertebra 4.

kinks (Fig. 2G,G′). The two types of abnormal vertebrae could be found in the same individual, with the bow tie shape more frequent in the sacral region. We conclude that *Tsg* is not an essential gene for embryogenesis and that its inactivation causes dwarfism, vertebral abnormalities and osteoporosis detectable by X-rays.

Defective chondrogenesis in the caudal region of *Tsg*$^{-/-}$ embryos

We next analyzed the pathogenesis of the vertebral defects (Fig. 3). Formation of the vertebral column is the result of several inductive events. First, the notochord induces differentiation of somitic mesoderm into sclerotome. After migrating next to the notochord, sclerotomal cells form an unsegmented perichordal tube, which is then subdivided into alternate condensed and uncondensed areas of mesenchyme (Grüneberg, 1963; Theiler, 1988). The condensed areas give rise to the annulus or future intervetebral disc. The annulus separates into a fibrous outer part (annulus fibrosus) and an inner part of prechondrogenic mesenchyme (inner annulus), forming concentric rings around the notochord. The uncondensed areas give rise to the cartilaginous primordia of the vertebral bodies. Finally, the notochord disappears from the developing vertebral body (possibly extruded by the increasing pressure of the cartilage extracellular matrix) but remains at the center of the intervertebral disc, where it forms the nucleus pulposus (Grüneberg, 1963; Theiler, 1988; Aszodi et al., 1998).

At E12.5, the morphology of the somites, sclerotomes and areas of condensed and uncondensed mesenchyme was similar in wild-type and *Tsg*$^{-/-}$ animals (Fig. 3A,A′). However, by E15.5, the *Tsg*$^{-/-}$ vertebral column showed distinct abnormalities. In the wild-type tails, the round vertebral bodies formed a core of differentiated chondrocytes flanked by proliferating chondrocyte precursors (Fig. 3B). Notochordal cells were mostly excluded from the vertebral bodies and accumulated in the intervertebral regions to form the nucleus pulposus (Fig. 3B). In the *Tsg*$^{-/-}$ tail, the vertebral bodies were narrower and rectangular with fewer differentiated chondrocytes, while the intervertebral regions were expanded and had fewer proliferating chondrocyte precursors (Fig. 3B′). The notochordal cells were not resorbed from vertebral bodies, and a distinctive nucleus pulposus was not formed (Fig. 3B′). These observations indicated impaired chondrocyte differentiation. The decrease of vertebral body cartilage, increase in intervertebral tissue and persistence of the notochord was confirmed by Alcian Blue staining (Fig. 3C,C′).

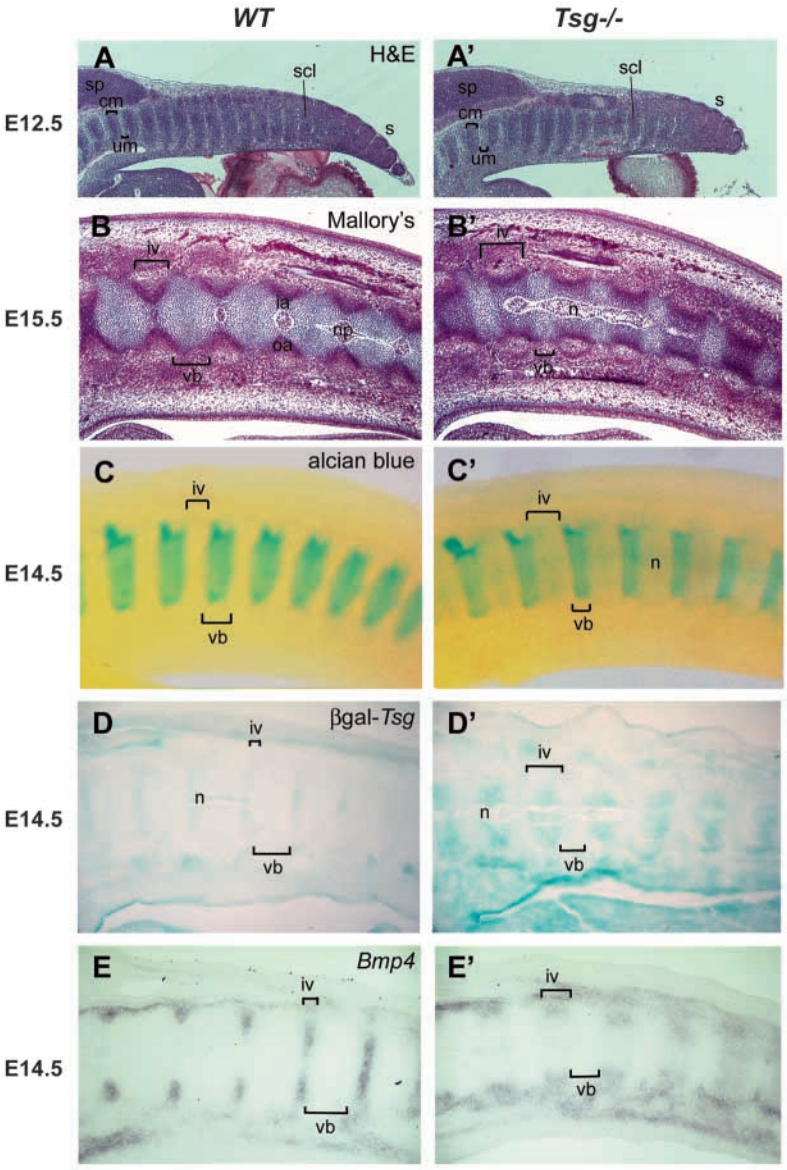

Fig. 3. Development of vertebral defects in *Tsg* mutant embryos. (A-A′) Hematoxylin and Eosin staining of sagittal sections of the tail of E12.5 wild-type and $Tsg^{-/-}$ embryos. (B-B′) Mallory's tetrachrome staining of sagittal sections of E15.5 wild-type and $Tsg^{-/-}$ tails. Vertebral bodies (vb); intervertebral regions (iv) consisting of an outer annulus (oa) and inner annulus (ia); nucleus pulposus (np) containing the remnants of the notochord. In the wild type, the np is surrounded by the prechondrogenic mesenchyme of the ia. (B′) The *Tsg* mutant vertebral bodies are more rectangular and narrower than wild type; the intervertebral region is expanded, notochordal cells are not resorbed in the vertebral bodies. (C-C′) Alcian Blue staining of E14.5 wild-type and $Tsg^{-/-}$ embryos. Note the smaller vertebral bodies and persistence of the notochord (n) in the mutant. (D-D′) β-gal staining of the tail region of E14.5 wild-type and $Tsg^{-/-}$ embryos showing expanded *Tsg* expression in intervertebral prechondrogenic mesenchyme and in the notochord of the mutant. (E-E′) Expression of *Bmp4* at E14.5 in wild-type and $Tsg^{-/-}$ embryos. (E) *Bmp4* is expressed in the intervertebral annulus fibrosus, which is expanded in the mutant (E′). cm, condensed mesenchyme; scl, sclerotome; s, somite; um; uncondensed mesenchyme; sp, spinal chord.

The expression of *Tsg* (visualized by β-gal activity) and *Bmp4* confirmed the expansion of the intervertebral region with respect to the vertebral bodies at E14.5 and E13.5 (Fig. 3D,D′,E,E′; data not shown). *Tsg* expression was observed in the notochord and in the condensed mesenchyme of the inner annulus (Fig. 3D; data not shown). *Bmp4* was expressed in the annulus fibrosus of the intervertebral region (Fig. 3E). Both intervertebral region markers were expanded in $Tsg^{-/-}$, while vertebral bodies were decreased (Fig. 3D′,E′). We conclude that chondrocyte differentiation is impaired in $Tsg^{-/-}$ mutants. As Bmp signaling is crucial for cartilage formation and several *Bmp* mutants display skeletal defects (Kingsley, 1994; Karsenty, 2000; Canalis et al., 2003), these observations could be considered consistent with a positive role for Tsg in Bmp signaling during vertebral differentiation.

Holoprosencephaly in $Tsg^{-/-};Bmp4^{+/-}$ mutants

We next asked whether *Tsg* and *Bmp4* interact genetically. Homozygous null mutants for *Bmp4* die around gastrulation (Winnier et al., 1995). Heterozygous *Bmp4* animals are viable and display craniofacial malformations, microphthalmia, cystic kidney and preaxial polydactily (Dunn et al., 1997). Matings were set up between $Tsg^{+/-};Bmp4^{+/-}$ and $Tsg^{+/-};Bmp4^{+/+}$ animals in B6SJL/F1 background. No additional phenotypes, compared with the ones already described, were detected in $Tsg^{+/-};Bmp4^{+/-}$ or $Tsg^{-/-};Bmp4^{+/+}$ littermates. However, $Tsg^{-/-};Bmp4^{+/-}$ neonates displayed severe head malformations (Fig. 4) with a 64% penetrance (seven out of 11 $Tsg^{-/-};Bmp4^{+/-}$, n=77). In severe cases, a single nostril, lack of mouth opening, anophtalmia and low implantation of the external ears were observed (Fig. 4A,A′). Histological sections of the snout region showed the absence of nasal septum, lower mandible and tongue (Fig. 4B,B′), the latter two being derivatives of the first branchial arch. Similar phenotypes were observed at E15.5 (Fig. 5A′).

$Tsg^{-/-};Bmp4^{+/-}$ mutant embryos presented severe malformations of the prosencephalon. First, the telencephalon formed a single cavity (instead of two lateral vesicles), owing to the absence of the medial wall (Fig. 5C,C′). This malformation is known as holoprosencephaly. Second, the lateral ganglionic eminence or striatum, which gives rise to the basal nuclei (caudate, putamen and pallidum) of the telencephalon was completely absent (Fig. 5B′,C′). Third, the basal diencephalon was greatly thickened at the level of the hypothalamus (Fig. 5B,B′). Finally, after the initial formation of an optic vesicle, the retina and lens did not develop in $Tsg^{-/-};Bmp4^{+/-}$ embryos, despite the presence of an orbit and upper and lower eyelids (Fig. 5B,B′ and data not shown). Cyclopia was not observed. The anophthalmia observed was more severe than the $Bmp4^{+/-}$ microphthalmia (Dunn et al., 1997). Because in $Tsg^{-/-}$ the main phenotype was observed in

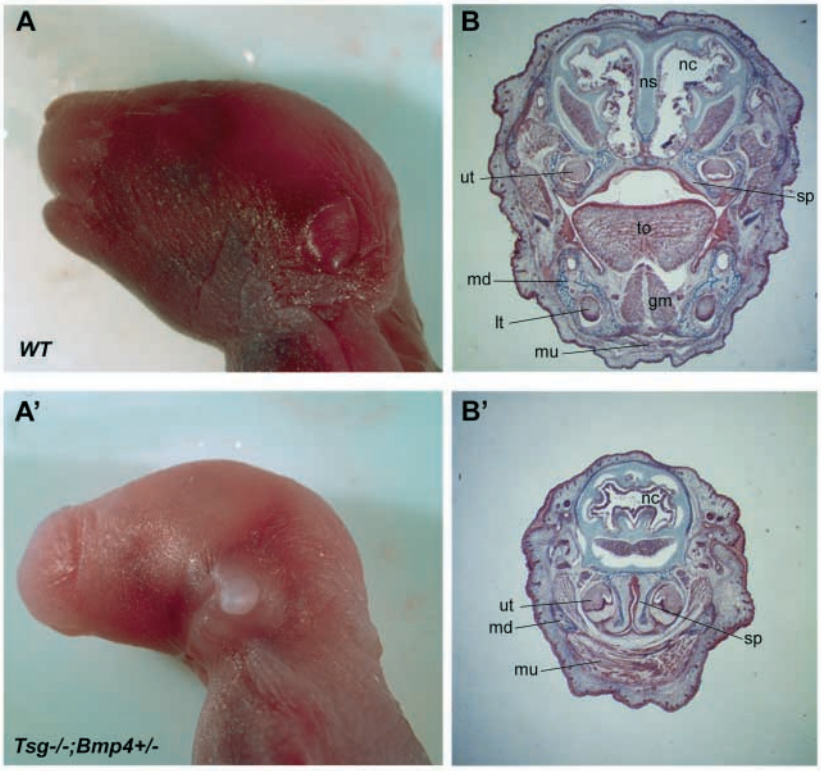

Fig. 4. *Tsg*$^{-/-}$;*Bmp4*$^{+/-}$ neonates display holoprosencephaly. (A-A′) Lateral view of the heads of wild-type and *Tsg*$^{-/-}$;*Bmp4*$^{+/-}$ newborn mice. *Tsg*$^{-/-}$ or *Bmp4*$^{+/-}$ are indistinguishable from wild type. The *Tsg*$^{-/-}$;*Bmp4*$^{+/-}$ mutant lacks a mouth opening, has only one nostril, and the external ear has an abnormal setting. (B-B′) Frontal sections through the snout region of the same neonates stained with Mallory's tetrachrome. The lack of nasal septum (ns) indicates holoprosencephaly. The lower jaw is reduced. gm, genioglossus muscle; lt, lower tooth; md, mandible; mu, muscle; nc, nasal cavity; sp, secondary palate; to, tongue; ut; upper tooth.

the tail vertebrae, we paid particular attention to enhancing or suppressing effects in the caudal region of *Tsg*$^{-/-}$;*Bmp4*$^{+/-}$ animals. However, we could not detect any differences with *Tsg*$^{-/-}$ embryos, indicating that the effects of Tsg on vertebral development may be caused by interactions with Bmps other than Bmp4. We also examined the kidney histologically, which can develop cysts in *Bmp4*$^{+/-}$, and failed to find genetic interactions. We conclude that the reduction of *Bmp4* gene dose by one half in *Tsg*$^{-/-}$;*Bmp4*$^{+/-}$ embryos leads to holoprosencephaly, lack of basal ganglia and eyes.

Comparison of the expression of *Tsg* and *Bmp4*

In light of the phenotypes uncovered by genetic interactions between *Tsg* and *Bmp4*, we examined the expression of *Tsg* in comparison to that of *Bmp4* and *Chd*, specifically in the affected structures (Fig. 6). At E8.0 *Tsg*, *Bmp4* and *Chd* are expressed in adjacent domains in anterior regions. *Tsg* was diffusely expressed in ventral neuroectoderm, head mesoderm and foregut endoderm (Fig. 6A, Fig. 1I,J). At this stage *Bmp4* was expressed in the surface ectoderm surrounding the neural folds and in extra-embryonic mesoderm (Fig. 6B,C) (Lawson et al., 1999; Fujiwara et al., 2002). *Chd* was expressed in the notochord, prechordal plate and dorsal endoderm (Fig. 6D) (Bachiller et al., 2003). The Tld proteases that regulate Chd activity have broad expression patterns, which include the neuroectoderm and extra-embryonic tissues (Scott et al., 1999). *Tsg* expression continued to be diffuse at later stages, with ventral brain, eye, branchial arches, limb buds and ventral posterior mesoderm expressing *Tsg* at higher levels (Fig. 6E,G, Fig. 1H,H′). *Bmp4* was expressed in dorsal telencephalon, eye, proximal ectoderm of the first branchial arch, frontonasal mass, maxillary arch and limb buds, ventral-posterior mesoderm and allantois (Fig. 6F,H). *Chd* is expressed in pharyngeal endoderm at these stages, and at low levels in the first branchial arch (Stottmann et al., 2001; Bachiller et al., 2003). We conclude that the genetic interactions between *Bmp4* and *Tsg* produce phenotypes in regions in which both genes are expressed in adjacent domains, such as the forebrain and the eye. However, other regions in which the expression domains show strong overlap, such as ventral mesoderm and limb buds, do not show additional phenotypes. Presumably in these regions other Bmps compensate for the decreased level of *Bmp4*. One region in which expression of *Bmp4* overlaps with *Tsg* and produces dose-dependent phenotypes is the first branchial arch.

First branchial arch defects in *Tsg*$^{-/-}$;*Bmp4*$^{+/-}$ embryos

The first branchial arch becomes apparent at E8.25 and then subdivides into the mandibular and maxillary components. After outgrowth and fusion at the midline, they give rise to many structures, such as the jaws, tongue and teeth. Some of these elements were absent or reduced in *Tsg*$^{-/-}$;*Bmp4*$^{+/-}$ embryos (Fig. 4B′). *Tsg* is expressed in all branchial arches, whereas *Bmp4* is expressed in the surface ectoderm of the maxillary and mandibular arches (Fig. 6F,H), in which phenotypes were observed. The hyoid arch does not express *Bmp4* and was unaffected [in *Chd* mutants the hyoid arch and most of the hyoid bone are missing (Bachiller et al., 2003)]. We used two markers, *Dlx5* and *Fgf8*, to follow the development of the first arch. *Dlx5* is a homeobox gene expressed in the mandibular component of the first branchial arch and in the hyoid arch at E10.5 (Acampora et al., 1999) (Fig. 7A). *Dlx5* is required for first branchial arch development and is a downstream target of Bmp4 signals (Miyama, 1999). In the *Tsg*$^{-/-}$;*Bmp4*$^{+/-}$ embryo shown in Fig. 6A′, the mandibular arch, marked by *Dlx5* expression, was absent on the right side and reduced on the left. *Fgf8* is a member of the fibroblast growth factor family that is required for the patterning of the first branchial arch (Trumpp et al., 1999; Abu-Issa et al., 2002). *Fgf8*, is expressed in the rostral surface ectoderm of the first arch at E8.5 (Fig. 7B). In *Tsg*$^{-/-}$;*Bmp4*$^{+/-}$ embryos the first arch was not distinguishable and *Fgf8* expression was lost (Fig. 7B′). Thus, it appears that in the compound mutant the mandibular component of the first arch is reduced or fails to develop. We conclude that Tsg

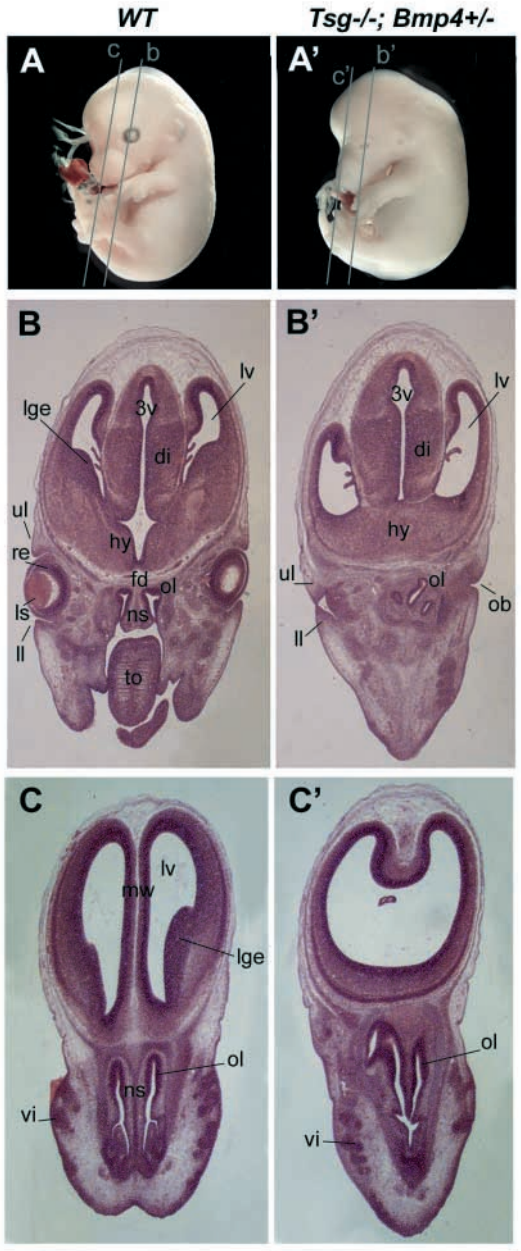

Fig. 5. Holoprosencephaly in *Tsg*$^{-/-}$;*Bmp4*$^{+/-}$ embryos at E15.5. (A-A′) E15.5 wild-type and *Tsg*$^{-/-}$;*Bmp4*$^{+/-}$ embryos. The plane of sections shown below are designated b,b′,c and c′. (B,B′,C,C′) Histological sections were stained with Hematoxylin and Eosin. The lateral ganglionic eminence (lge) is missing and the floor of the diencephalon (fd) is greatly thickened in the mutant. Note the fusion of the lateral ventricles, owing to the lack of a medial wall (mw) and the lack of nasal septum (ns). In addition, note the empty orbits (ob), lack of lens (ls) and retina (re) of the eyes. di, diencephalon; hy, hypothalamus; ll, lower lid; lv, lateral ventricle; ol, olfactory epithelium; to, tongue; ul, upper lid; vi, follicles of vibrissae; 3V, third ventricle.

and Bmp4 cooperate in the development of the first branchial arch.

Onset of head defects in *Tsg*$^{-/-}$;*Bmp4*$^{+/-}$ embryos

Several signaling centers have been implicated in specific steps of forebrain development during embryogenesis. The anterior visceral endoderm (AVE) plays an early role, and later on the prechordal plate (PCP), the anterior neural ridge (ANR) and the midbrain-hindbrain isthmus further refine the pattern (Rubenstein et al., 1998; Beddington and Robertson, 1999). To analyze the onset of the holoprosencephaly in *Tsg*$^{-/-}$;*Bmp4*$^{+/-}$ embryos, specific markers expressed in these signaling centers were analyzed between E7.5 and E8.5. *Fgf8* is expressed in the ANR, the isthmus, the pharyngeal endoderm and the tailbud before the embryo turns (Crossley and Martin, 1995; Abu-Issa et al., 2002; Garel et al., 2003) (Fig. 7C), and in the commissural plate, the first branchial arch in addition to the isthmus and the tailbud after the turning of the embryo (Fig. 7B). No differences were found in the initial expression of *Fgf8* in the *Tsg*$^{-/-}$;*Bmp4*$^{+/-}$ mutants (Fig. 7C′), but at E8.5 the commissural plate and corresponding staining were missing (asterisk in Fig. 7B′). *Shh* is a secreted signaling factor expressed in the embryonic midline (notochord and prechordal plate) (Chiang et al., 1996). At E8.5, *Shh* expression is also seen in the basal plate of the telencephalon, diencephalon and mesencephalon (McMahon et al., 1998) (Fig. 7D). In *Tsg*$^{-/-}$;*Bmp4*$^{+/-}$ embryos, *Shh* expression was lost in the basal telencephalon and diencephalon but persisted in the basal mesencephalon at E8.5 (Fig. 7D′). *Six3* expression marks the developing telencephalic territory in the neural plate (Oliver et al., 1995) and was moderately reduced in mutant embryos at E8.0 (data not shown). During gastrulation, the AVE appeared normal in *Tsg*$^{-/-}$;*Bmp4*$^{+/-}$ embryos, as judged by the specific marker *Cer1* at E6.5 (Belo et al., 1997) (Fig. 7E,E′). The anterior endoderm and node marker *Hex* was normal at E7.5, a stage in which it marks both primitive and definitive endoderm (Thomas et al., 1998) (Fig. 7F,F′).

We conclude that *Tsg* inactivation combined with half the normal dose of Bmp4 results in the loss of *Shh* and *Fgf8* expression in the basal telencephalon and diencephalon. Although the absence of these important signaling molecules could suffice to explain the observed holoprosencephaly, a small decrease of the forebrain territory was already observed at the neural plate stage. Formation of the AVE and ANR appeared normal in the compound mutant embryos. The holoprosencephaly phenotype in *Tsg*$^{-/-}$;*Bmp4*$^{+/-}$ embryos arose around E8.0, concomitantly with the loss of *Shh* and *Fgf8* expression. The results indicate that Tsg is required for the proper function of Bmp4 in the formation of the telencephalic vesicles.

Discussion

The secreted factor Tsg exhibits multiple biochemical activities in the Bmp pathway. Depending on the context, *Tsg* results in Bmp-promoting or anti-Bmp effects. We have examined *Tsg* loss of function by targeting the *Tsg* gene in the mouse and by analyzing the genetic interaction between the *Tsg* and *Bmp4* loci. *Tsg* inactivation resulted in viable homozygous mutants of reduced size displaying minor skeletal malformations. However, when in addition one copy of the *Bmp4* gene was removed, the *Tsg*$^{-/-}$;*Bmp4*$^{+/-}$ mutants displayed significant defects in forebrain, eye and branchial arch formation. The strong enhancement of *Bmp4* haploinsufficiency in *Tsg*$^{-/-}$

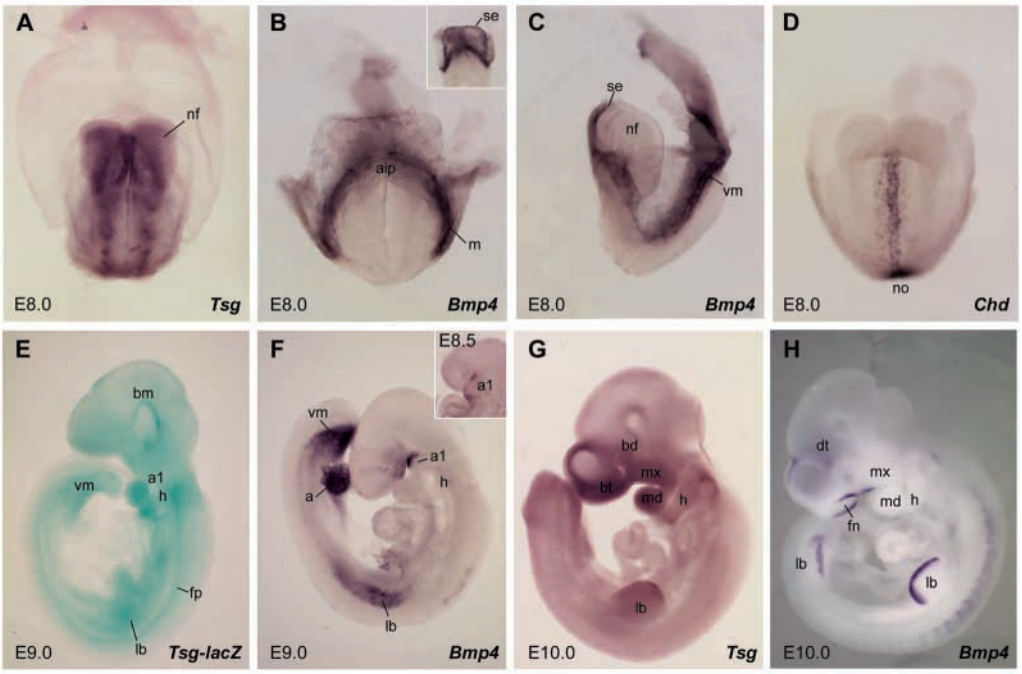

Fig. 6. Comparative expression of *Tsg*, *Bmp4* and *Chd*. Whole-mount in situ hybridization was performed between E8.0 and E10.0 using the gene markers indicated. (A) Tsg expression at E8.0, frontal view. (B,C) Frontal and lateral views of *Bmp4* expression at E8.0. Inset shows expression in the surface ectoderm (se) at E7.75. (D) *Chd* expression at E8.0 in the node (no), notochord, prechordal plate and endoderm. (E) β-Gal staining showing diffuse expression of *Tsg* at E9.0. (F) Expression of *Bmp4* at E9.0. Inset shows expression in the branchial arch as early as E8.5. (G) Expression of *Tsg* at E10.0. (H) Expression of *Bmp4* at E10.0. a, allantois; a1, first branchial arch; aip, anterior intestinal portal; bd, basal diencephalon; bm, basal mesencephalon; bt, basal telencephalon; dt, dorsal telencephalon; fn, frontonasal process; fp, floor plate; h, hyoid arch; lb, limb bud; m, mesoderm; md, mandibular; mx, maxillary; nf, neural fold; vm, ventral mesoderm.

mutants supports the view that Tsg promotes Bmp4 activity in vivo.

Tsg is not essential for embryogenesis

Tsg has been conserved in evolution between *Drosophila* and the vertebrates and is known to bind in vitro several Bmps, such as Bmp2, Bmp4 and Bmp7, as well as the Bmp antagonist Chd (Oelgeschläger et al., 2000; Chang et al., 2001; Scott et al., 2001). Nosaka et al. (Nosaka et al., 2003) recently generated a larger deletion of the *Tsg* gene that resulted in a similar phenotype to the one described here. In addition, they reported a lethality of up to 50% of the mutants in the first month, which we did not observe. This discrepancy may be due to a difference in genetic backgrounds (inbred C57BL/6 versus the hybrid B6SJL/F1 background used here). Mouse *Tsg* had been cloned as a gene that is differentially expressed in the thymus (Graf et al., 2001; Graf et al., 2002). Nosaka et al. (Nosaka et al., 2003) identified severe deficiencies in thymocyte cell number and differentiation in $Tsg^{-/-}$ mice, which were interpreted to indicate an increase in Bmp signaling. The thymus phenotype was not analyzed here. As discussed in the introduction, Tsg has both Bmp-promoting and anti-Bmp properties, depending on the presence of Chd and Tld. Tsg facilitates the formation of ternary complexes with Bmp and Chd and in this way inhibits Bmp signaling through its cognate receptors (De Robertis et al., 2000) until Chd is cleaved by Tld (Larrain et al., 2001). The presence of Tsg facilitates proteolytic cleavage of Chd by Tld, promoting Bmp activity. Microinjection of antisense morpholino oligos in zebrafish and *Xenopus* have provided evidence that Tsg can inhibit Bmp signaling and that it cooperates with Chd in this function, presumably by interfering with ternary complex formation (Ross et al., 2001; Blitz et al., 2003). Tsg mutant proteins that are unable to bind Bmp4 can still bind to Chd and other CR-containing proteins and have potent Bmp-promoting activity (Oelgeschläger et al., 2003a). The multiple functions of Tsg made it particularly important to analyze its function in defined genetic situations.

Despite its strong evolutionary conservation, Tsg was not required for vertebrate embryonic development. In *Drosophila*, *Tsg* mutation results in the loss of the amnioserosa a tissue that requires highest Bmp/Dpp activity (Mason et al., 1994). Mutation of *Drosophila Tsg* results in the lack of peak phosphorylation of the transcription factor Mad (Ross et al., 2001) and in the inability of Dpp to diffuse in the embryo (Eldar et al., 2002). A second Tsg gene, *Drosophila Tsg2* (L. Marsh, communication to FlyBase FBgn0000394) is affected in the *crossveinless* (*cv*) mutant. *cv* causes a loss of the posterior crossveins (Bridges, 1920), a structure that requires maximal Bmp signaling in the *Drosophila* wing. In addition, a third *Tsg* homolog was identified, *Drosophila Tsg3*, which only contains the C-terminal half of the protein (Vilmos et al., 2001). *Drosophila Tsg3* maps close to *shrew*, a gene also required to achieve highest signaling levels in the Bmp/Dpp dorsoventral signaling gradient (Vilmos et al., 2001; Ferguson and Anderson, 1992). Although the mouse genome has been sequenced, genes with small exons can escape a BLAST search. It is conceivable that additional *Tsg* homologues may exist in the mouse genome; in *Xenopus* a divergent *xTsg2* cDNA with biological activities similar to those of *Xenopus* Tsg has been recently isolated (M. Oelgeschläger, U. Tran and E.M.D.R., unpublished).

Tsg function in skeletal development

The loss of *Tsg* in mouse resulted in vertebral abnormalities. The neural arches of the cervical and thoracic vertebrae fail to fuse at the midline and kinked tails were observed. We examined the pathogenesis of the vertebral defects in *Tsg*

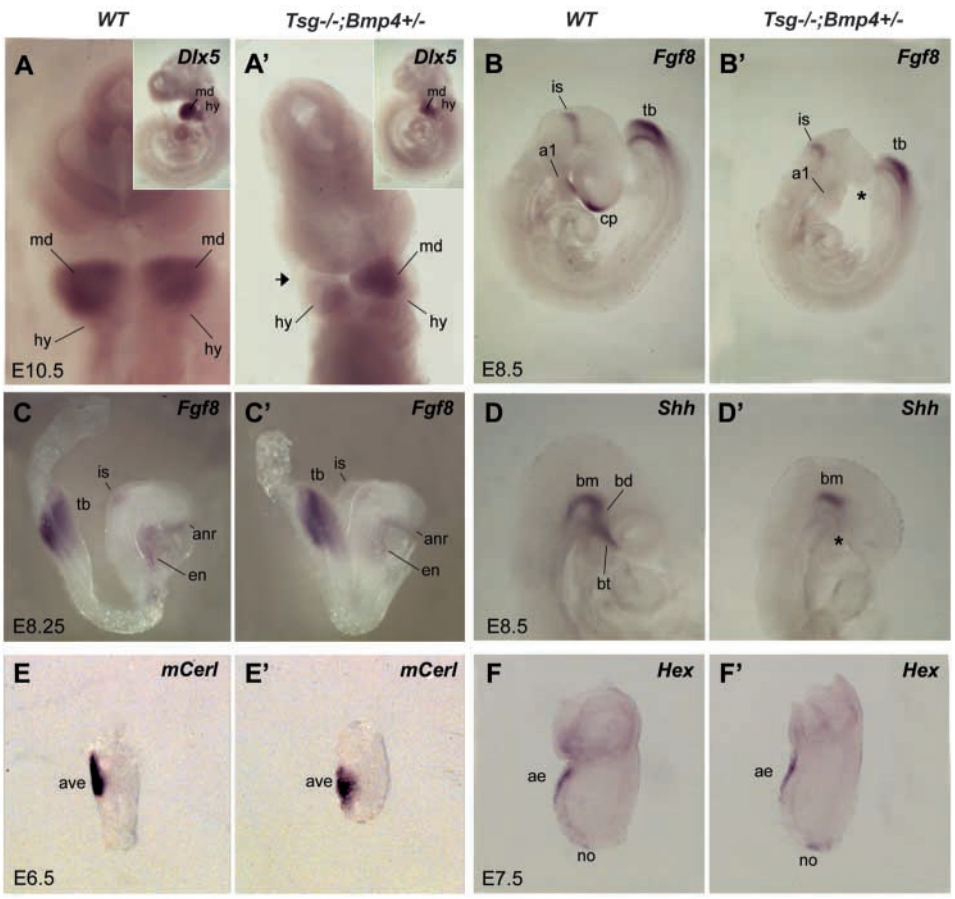

Fig. 7. Defective development of telencephalic vesicles and first pharyngeal arch in *Tsg*$^{-/-}$;*Bmp4*$^{+/-}$ embryos. The phenotypes of *Tsg*$^{-/-}$ and *Bmp4*$^{+/-}$ were indistinguishable from wild-type. (A-A′) Frontal view of E10.5 embryos stained with *Dlx5*. Insets show lateral views. The right mandibular component of the first arch is missing in the compound mutant (arrow). hy, hyoid arch; md, mandibular component of the first pharyngeal arch. (B,B′,C,C′) Lateral view of E8.5 and E8.25 embryos hybridized with *Fgf8*. (B) At E8.5 *Fgf8* is expressed in the proximal ectoderm of the first pharyngeal arch (a1), isthmus (is), commissural plate (cp) and tailbud (tb). (B′) Expression in the pharyngeal arch and the commissural plate (indicated by an asterisk) is missing in the mutant. (C-C′) At E8.25, *Fgf8* is present in the anterior neural ridge (anr), isthmus, pharyngeal endoderm (en) and tailbud; no differences in *Fgf8* expression were observed at this stage. (D-D′) At E8.5 *Shh* is expressed in the basal mesencephalon (bm), basal diencephalon (bd) and basal telencephalon (bt) and the notochord. Expression in the basal diencephalon and basal telencephalon is missing in the mutant (asterisk). (E-E′). Expression of mouse *Cer1* in the anterior visceral endoderm (ave) of wild-type and *Tsg*$^{-/-}$;*Bmp4*$^{+/-}$ embryos at E6.5. (F-F′) Expression of *Hex* in the anterior endoderm (ae) and node (no) of wild-type and *Tsg*$^{-/-}$;*Bmp4*$^{+/-}$ embryos at E7.5.

mutants. Instead of a single ossification center in caudal vertebrae, *Tsg*$^{-/-}$ animals develop two independent centers. Although in most cases the twin centers ultimately fuse, in some vertebrae one of them fails to develop. The end result is a wedge-shaped hemi-vertebra that leads to an abnormal angle between neighboring vertebral articulations, causing the tail kinks (Fig. 2G′). Tail kinks are frequently observed in mouse skeletal mutants (Grüneberg, 1963; Theiler, 1988) and can originate from defects in sclerotome differentiation. In *Tsg*$^{-/-}$ mice, the cartilage of the vertebral bodies was reduced and the inner annulus, which expresses *Tsg*, failed to differentiate pre-chondrogenic cells.

As Bmps are known to promote cartilage differentiation (Erlebacher et al., 1995; Hogan, 1996; Canalis et al., 2003), Tsg could be viewed as promoting Bmp activity in this tissue. Other components of the Chd/Tsg/Bmp/Tld regulatory pathway are also expressed in the developing skeleton (Scott et al., 1999) and in particular *Chd* is found in the outer annulus (Coffinier et al., 2002). Although *Bmp4* is also expressed in the outer intervertebral annulus, no increase in the severity of the tail phenotype was found in *Tsg*$^{-/-}$;*Bmp4*$^{+/-}$ mutants. However, other Bmps expressed in the tail region may have redundant functions with *Bmp4*. Of particular interest is *Bmp7*, as *Bmp7* mutant mice have kinked tails (Dudley et al., 1995; Jena et al., 1997). The analysis of the genetic interactions between *Chd*, *Bmp7* and *Tsg* in the mouse, are currently under investigation in our laboratory. Preliminary results indicate that *Tsg* cooperates with *Bmp7* in the differentiation of ventral embryonic structures (L.Z., K. Lyons and E.M.D.R., unpublished).

Tsg$^{-/-}$ adult mice present osteoporosis, which has been interpreted as a loss of Bmp signaling (Nosaka et al., 2003). Although there is much evidence linking Bmp signals to cartilage formation, a role for Bmps in bone differentiation is less firmly established (Karsenty, 2000). However, more recent studies in transgenic mice overexpressing a dominant-negative Bmp receptor or Noggin (Nog), in bone indicate that Bmps are required for postnatal bone growth (Zhao et al., 2002; Devlin et al., 2003).

Tsg interacts with *Bmp4*

Tsg interacts genetically with *Bmp4*. Biochemical studies had shown a direct interaction between Tsg and Bmps, but a genetic demonstration that these molecules function in the same pathway in vivo was lacking, even in *Drosophila*. We chose Bmp4 because of the direct biochemical interactions between the two proteins and for the strong *Bmp4* loss-of-function phenotype in mouse. *Bmp4* homozygous mutants die at gastrulation (Winnier et al., 1995), whereas *Bmp4*$^{+/-}$ mice present mild haploinsufficient phenotypes with variable penetrance, making it a particularly suitable model for uncovering potential genetic interactions (Dunn et al., 1997).

Tsg$^{-/-}$;*Bmp4*$^{+/-}$ animals did not survive beyond birth and presented additional phenotypes to those already found in either *Tsg*$^{-/-}$ or *Bmp4*$^{+/-}$ animals (Fig. 5). First, the forebrain presented reduced telencephalic vesicles that fused into a single ventricular cavity, the defining characteristic of holoprosencephaly (Muenke and Beachy, 2000). Second, eye vesicles were formed initially but degenerated, although the orbits and eyelids still differentiated. This phenotype suggests an enhancement of the *Bmp4*$^{+/-}$ phenotype since microphthalmia can result from *Bmp4* haploinsufficiency (Dunn et al., 1997). Recently, anophthalmia has been described in mutant mice with hypomorphic alleles of *Bmp4* (Kulessa and Hogan, 2002) and in *Cre-Foxg1;Bmp4*$^{loxP\text{-}lacZ\text{-}neo}$ mutants that lack *Bmp4* expression in the telencephalon (Hebert et al., 2002; Hebert et al., 2003). *Bmp4* and *Tsg* are strongly expressed in the eye region (Figs 1 and 6). In addition, *Bmp4* is essential for lens induction (Furuta and Hogan, 1998) and lenses were not observed in compound mutants. Third, the lateral ganglionic eminence of the basal telencephalon did not form. Fourth, the floor of the diencephalon was greatly thickened a site of co-expression for *Bmp4* (Furuta et al., 1997) and *Tsg* (Fig. 1J).

Finally, the mandibular component of the first branchial arch was hypoplastic or absent in the compound mutants. Both *Bmp4* and *Tsg* are expressed in the developing branchial arch (Fig. 6). A first branchial arch phenotype was described in *Cre-Foxg1;Bmp4*$^{loxP\text{-}lacZ\text{-}neo}$ mutants (Hebert et al., 2003). Of all the phenotypes of *Tsg*$^{-/-}$;*Bmp4*$^{+/-}$ animals, the only one not previously reported in *Bmp4* mutations was the holoprosencephaly. It may appear surprising that *Cre-Foxg1;Bmp4*$^{loxP\text{-}lacZ\text{-}neo}$ mutants that lack *Bmp4* in the forebrain do not have this phenotype. However, our results show that the onset of the holoprosencephaly occurs earlier than the recombination induced by *Cre-Foxg1* mice (Hebert et al., 2003). It is thus likely that *Bmp4* is required for the development of the telencephalic vesicles prior to E8.5, which would not have been revealed in the conditional *Cre-Lox* approach (Hebert et al., 2003). In conclusion, *Tsg*$^{-/-}$;*Bmp4*$^{+/-}$ mutants present phenotypes similar to those observed in *Bmp4* hypomorphic and loss-of-function mutants.

Tsg, *Bmp4* and holoprosencephaly (HPE)

The human *Tsg* gene maps close to the *HPE* locus 4 on chromosome 18p11.3 (Graf et al., 2001). However no mutations in the human *Tsg* gene could be detected in familial cases of HPE at locus 4 (M. Muenke and E.M.D.R., unpublished observations). It has been proposed in the multi-hit hypothesis that sporadic HPE may result from mutations in more than one gene (Ming and Muenke, 2002). This is what is observed in our study, in which HPE requires mutations in two genes, *Tsg* and *Bmp4*, to become manifest. However, we have recently observed sporadic cases of HPE in *Tsg*$^{-/-}$ embryos in mice that had been bred for six generations into B6SJL/F1 background. Importantly, these *Tsg*$^{-/-}$ embryos with HPE still developed eyes, whereas *Tsg*$^{-/-}$;*Bmp4*$^{+/-}$ had HPE with anophthalmia. In earlier crosses, the ones reported in this paper, we only observed HPE in *Tsg*$^{-/-}$ embryos when one copy of *Bmp4* was removed. It is likely that a genetic modifier of unknown nature was changed by breeding in the laboratory.

Tsg and *Bmp4* are expressed in adjacent or overlapping regions (Figs 1 and 6). The holoprosencephalic phenotype of the *Tsg*$^{-/-}$;*Bmp4*$^{+/-}$ mutants is not of early onset, for the anterior visceral endoderm and the anterior neural ridge were normally formed. At E8.5 the expression of two crucial signaling factors, *Fgf8* and *Shh*, was defective in *Tsg*$^{-/-}$;*Bmp4*$^{+/-}$ embryos and this can explain the phenotypes observed. *Shh* is required for the growth of the ventral forebrain and when mutated causes a more severe HPE than the one described here since it includes cyclopia (Chiang et al., 1996; Ishibashi and McMahon, 2002). In addition, *Shh*$^{-/-}$ mice fail to express *Fgf8* in the ventral forebrain (Ohkubo et al., 2002). *Fgf8* null embryos die at gastrulation (Sun et al., 1999), but the study of *Fgf8* hypomorphic alleles has demonstrated its requirement for forebrain formation (Meyers et al., 1998; Garel et al., 2003) and first branchial arch development (Trumpp et al., 1999; Abu-Issa et al., 2002).

Multiple experiments in mouse and chick embryos have shown that signals from Bmps, Shh and Fgf8 regulate the growth of the telencephalon through proliferation and cell death (Furuta et al., 1997; Rubenstein et al., 1998; Anderson et al., 2002; Ohkubo et al., 2002; Storm et al., 2003). For example, the implantation of Bmp4-coated beads causes HPE (Furuta et al., 1997; Ohkubo et al., 2002). Ectopic expression of *Bmp4* and *Bmp5* in the chick forebrain causes cyclopia and HPE (Golden et al., 1999). *Chd*;*Nog* double mutants, which should have increased Bmp signaling, also show HPE (Bachiller et al., 2000; Anderson et al., 2002). However, ectopic expression of the Bmp antagonist Nog also inhibits telencephalic growth (Ohkubo et al., 2002). Therefore, it appears that the growth of the forebrain requires a fine balance of Bmp, Fgf8 and Shh signaling and that both excessive and insufficient signaling can result in similar phenotypes (Ohkubo et al., 2002).

Is the HPE in *Tsg*$^{-/-}$;*Bmp4*$^{+/-}$ embryos indicative of a pro-Bmp4 or an anti-Bmp4 effect? This question can be answered by a simple genetic argument. In the absence of *Tsg*, two copies of *Bmp4* are compatible with normal head development. However, when in addition one copy of *Bmp4* is removed, development of the ventral forebrain and first branchial arch are impaired. We conclude from these dose-dependent genetic interactions that during head development Tsg is required to promote Bmp4 signaling.

We thank K. Lyons, E. Delot, C. Coffinier, B. Reversade, O. Wessely and A. Ikeda for critical reading of the manuscript; and Z. Unno, U. Tran and D. Geissert for technical help. Special thanks to K. Lyons for thoughtful advice. We thank B. Hogan for the *Bmp4* mutant mice. The probes used were kind gifts from B. Hogan, G. Oliver, A. McMahon, R. Beddington, G. Martin, D. Wilkinson and E. Boncinelli. This work was supported by the Howard Hughes Medical Institute, of which L.Z. is an associate and E.M.D.R. an investigator.

References

Abreu, J. G., Ketpura, N. I., Reversade, B. and de Robertis, E. M. (2002). Connective-tissue growth factor (CTGF) modulates cell signalling by BMP and TGF-beta. *Nat. Cell Biol.* **4**, 599-604.

Abu-Issa, R., Smyth, G., Smoak, I., Yamamura, K. and Meyers, E. N. (2002). Fgf8 is required for pharyngeal arch and cardiovascular development in the mouse. *Development* **129**, 4613-4625.

Acampora, D., Merlo, G. R., Paleari, L., Zerega, B., Postiglione, M. P., Mantero, S., Bober, E., Barbieri, O., Simeone, A. and Levi, G. (1999). Craniofacial, vestibular and bone defects in mice lacking the Distal-less-related gene Dlx5. *Development* **126**, 3795-3809.

Anderson, R. M., Lawrence, A. R., Stottmann, R. W., Bachiller, D. and Klingensmith, J. (2002). Chordin and noggin promote organizing centers of forebrain development in the mouse. *Development* **129**, 4975-4987.

Aszodi, A., Chan, D., Hunziker, E., Bateman, J. F. and Fassler, R. (1998). Collagen II is essential for the removal of the notochord and the formation of intervertebral discs. *J. Cell Biol.* **143**, 1399-1412.

Bachiller, D., Klingensmith, J., Kemp, C., Belo, J. A., Anderson, R. M., May, S. R., McMahon, J. A., McMahon, A. P., Harland, R. M., Rossant, J. et al. (2000). The organizer factors Chordin and Noggin are required for mouse forebrain development. *Nature* **403**, 658-661.

Bachiller, D., Klingensmith, J., Shneyder, N., Tran, U., Anderson, R., Rossant, J. and de Robertis, E. M. (2003). The role of Chordin/BMP signals in mammalian pharyngeal development and DiGeorge syndrome. *Development* **130**, 3567-3578.

Beddington, R. S. and Robertson, E. J. (1999). Axis development and early asymmetry in mammals. *Cell* **96**, 195-209.

Bedford, F. K., Ashworth, A., Enver, T. and Wiedemann, L. M. (1993). HEX: a novel homeobox gene expressed during haematopoiesis and conserved between mouse and human. *Nucleic Acids Res.* **21**, 1245-1249.

Belo, J. A., Bouwmeester, T., Leyns, L., Kertesz, N., Gallo, M., Follettie, M. and de Robertis, E. M. (1997). Cerberus-like is a secreted factor with neutralizing activity expressed in the anterior primitive endoderm of the mouse gastrula. *Mech. Dev.* **68**, 45-57.

Belo, J. A., Leyns, L., Yamada, G. and de Robertis, E. M. (1998). The prechordal midline of the chondrocranium is defective in Goosecoid-1 mouse mutants. *Mech. Dev.* **72**, 15-25.

Bridges, C. (1920). The mutant crossveinless in *Drosophila melanogaster*. *Proc. Natl. Acad. Sci. USA* **6**, 660-663.

Blitz, I. L., Cho, K. W. and Chang, C. (2003). Twisted gastrulation loss-of-function analyses support its role as a BMP inhibitor during early Xenopus embryogenesis. *Development* **130**, 4975-4988.

Canalis, E., Economides, A. N. and Gazzerro, E. (2003). Bone morphogenetic proteins, their antagonists, and the skeleton. *Endocrinol. Rev.* **24**, 218-235.

Chang, C., Holtzman, D. A., Chau, S., Chickering, T., Woolf, E. A., Holmgren, L. M., Bodorova, J., Gearing, D. P., Holmes, W. E. and Brivanlou, A. H. (2001). Twisted gastrulation can function as a BMP antagonist. *Nature* **410**, 483-487.

Chiang, C., Litingtung, Y., Lee, E., Young, K. E., Corden, J. L., Westphal, H. and Beachy, P. A. (1996). Cyclopia and defective axial patterning in mice lacking Sonic hedgehog gene function. *Nature* **383**, 407-413.

Coffinier, C., Ketpura, N., Tran, U., Geissert, D. and de Robertis, E. M. (2002). Mouse Crossveinless-2 is the vertebrate homolog of a Drosophila extracellular regulator of BMP signaling. *Mech. Dev.* **119S**, S179-S184.

Connors, S. A., Trout, J., Ekker, M. and Mullins, M. C. (1999). The role of tolloid/mini fin in dorsoventral pattern formation of the zebrafish embryo. *Development* **126**, 3119-3130.

Crossley, P. H. and Martin, G. R. (1995). The mouse Fgf8 gene encodes a family of polypeptides and is expressed in regions that direct outgrowth and patterning in the developing embryo. *Development* **121**, 439-451.

De Robertis, E. M., Larrain, J., Oelgeschläger, M. and Wessely, O. (2000). The establishment of Spemann's organizer and patterning of the vertebrate embryo. *Nat. Rev. Genet.* **1**, 171-181.

Devlin, R. D., Du, Z., Pereira, R. C., Kimble, R. B., Economides, A. N., Jorgetti, V. and Canalis, E. (2003). Skeletal overexpression of noggin results in osteopenia and reduced bone formation. *Endocrinology* **144**, 1972-1978.

Dudley, A. T., Lyons, K. M. and Robertson, E. J. (1995). A requirement for bone morphogenetic protein-7 during development of the mammalian kidney and eye. *Genes Dev.* **9**, 2795-2807.

Dunn, N. R., Winnier, G. E., Hargett, L. K., Schrick, J. J., Fogo, A. B. and Hogan, B. L. (1997). Haploinsufficient phenotypes in Bmp4 heterozygous null mice and modification by mutations in Gli3 and Alx4. *Dev. Biol.* **188**, 235-247.

Eldar, A., Dorfman, R., Weiss, D., Ashe, H., Shilo, B. Z. and Barkai, N. (2002). Robustness of the BMP morphogen gradient in Drosophila embryonic patterning. *Nature* **419**, 304-308.

Erlebacher, A., Filvaroff, E. H., Gitelman, S. E. and Derynck, R. (1995). Toward a molecular understanding of skeletal development. *Cell* **80**, 371-378.

Ferguson, E. L. and Anderson, K. V. (1992). Localized enhancement and repression of the activity of the TGF-beta family member, decapentaplegic, is necessary for dorsal-ventral pattern formation in the Drosophila embryo. *Development* **114**, 583-597.

Fujiwara, T., Dehart, D. B., Sulik, K. K. and Hogan, B. L. (2002). Distinct requirements for extra-embryonic and embryonic bone morphogenetic protein 4 in the formation of the node and primitive streak and coordination of left-right asymmetry in the mouse. *Development* **129**, 4685-4696.

Furuta, Y. and Hogan, B. L. (1998). BMP4 is essential for lens induction in the mouse embryo. *Genes Dev.* **12**, 3764-3775.

Furuta, Y., Piston, D. W. and Hogan, B. L. (1997). Bone morphogenetic proteins (BMPs) as regulators of dorsal forebrain development. *Development* **124**, 2203-2212.

Garel, S., Huffman, K. J. and Rubenstein, J. L. (2003). Molecular regionalization of the neocortex is disrupted in Fgf8 hypomorphic mutants. *Development* **130**, 1903-1914.

Golden, J. A., Bracilovic, A., Mc Fadden, K. A., Beesly, J. S., Rubenstein, J. L. and Grinspan, J. B. (1999). Ectopic bone morphogenetic proteins 5 and 4 in the chicken forebrain lead to cyclopia and holoprosencephaly. *Proc. Natl. Acad. Sci. USA* **96**, 2439-2444.

Graf, D., Timmons, P. M., Hitchins, M., Episkopou, V., Moore, G., Ito, T., Fujiyama, A., Fisher, A. G. and Merkenschlager, M. (2001). Evolutionary conservation, developmental expression, and genomic mapping of mammalian Twisted gastrulation. *Mamm. Genome* **12**, 554-560.

Graf, D., Nethisinghe, S., Palmer, D. B., Fisher, A. G. and Merkenschlager, M. (2002). The developmentally regulated expression of Twisted gastrulation reveals a role for bone morphogenetic proteins in the control of T cell development. *J. Exp. Med.* **196**, 163-171.

Grüneberg, H. (1963). *The Pathology of Development: A Study of Inherited Skeletal Disorders in Animals*. Oxford: Blackwell Scientific.

Hebert, J. M., Mishina, Y. and McConnell, S. K. (2002). BMP signaling is required locally to pattern the dorsal telencephalic midline. *Neuron* **35**, 1029-1041.

Hebert, J. M., Hayhurst, M., Marks, M. E., Kulessa, H., Hogan, B. L. and McConnell, S. K. (2003). BMP ligands act redundantly to pattern the dorsal telencephalic midline. *Genesis* **35**, 214-219.

Henrique, D., Adam, J., Myat, A., Chitnis, A., Lewis, J. and Ish-Horowicz, D. (1995). Expression of a Delta homologue in prospective neurons in the chick. *Nature* **375**, 787-790.

Hogan, B. L. (1996). Bone morphogenetic proteins: multifunctional regulators of vertebrate development. *Genes Dev.* **10**, 1580-1594.

Ishibashi, M. and McMahon, A. P. (2002). A sonic hedgehog-dependent signaling relay regulates growth of diencephalic and mesencephalic primordia in the early mouse embryo. *Development* **129**, 4807-4819.

Jegalian, B. G. and de Robertis, E. M. (1992). Homeotic transformations in the mouse induced by overexpression of a Hox3.3 transgene. *Cell* **71**, 901-910.

Jena, N., Martin-Seisdedos, C., McCue, P. and Croce, C. M. (1997). BMP7 null mutation in mice: developmental defects in skeleton, kidney, and eye. *Exp. Cell Res.* **230**, 28-37.

Karsenty, G. (2000). Bone morphogenetic proteins and skeletal and nonskeletal development. In *Skeletal Growth Factors* (ed. E. Canalis), pp. 291-298. Philadelphia: Lippincott Williams and Wilkins.

Kingsley, D. M. (1994). The TGF-beta superfamily: new members, new receptors, and new genetic tests of function in different organisms. *Genes Dev.* **8**, 995-1008.

Kulessa, H. and Hogan, B. L. (2002). Generation of a loxP flanked bmp4loxP-lacZ allele marked by conditional lacZ expression. *Genesis* **32**, 66-68.

Larrain, J., Bachiller, D., Lu, B., Agius, E., Piccolo, S. and de Robertis, E. M. (2000). BMP-binding modules in chordin: a model for signalling regulation in the extracellular space. *Development* **127**, 821-830.

Larrain, J., Oelgeschläger, M., Ketpura, N. I., Reversade, B., Zakin, L. and de Robertis, E. M. (2001). Proteolytic cleavage of Chordin as a switch for the dual activities of Twisted gastrulation in BMP signaling. *Development* **128**, 4439-4447.

Lawson, K. A., Dunn, N. R., Roelen, B. A., Zeinstra, L. M., Davis, A. M., Wright, C. V., Korving, J. P. and Hogan, B. L. (1999). Bmp4 is required for the generation of primordial germ cells in the mouse embryo. *Genes Dev.* **13**, 424-436.

Le Mouellic, H., Lallemand, Y. and Brulet, P. (1990). Targeted replacement of the homeobox gene Hox-3.1 by the Escherichia coli lacZ in mouse chimeric embryos. *Proc. Natl. Acad. Sci. USA* **87**, 4712-4716.

Marques, G., Musacchio, M., Shimell, M. J., Wunnenberg-Stapleton, K., Cho, K. W. and O'Connor, M. B. (1997). Production of a DPP activity gradient in the early Drosophila embryo through the opposing actions of the SOG and TLD proteins. *Cell* **91**, 417-426.

Mason, E. D., Konrad, K. D., Webb, C. D. and Marsh, J. L. (1994). Dorsal

midline fate in Drosophila embryos requires twisted gastrulation, a gene encoding a secreted protein related to human connective tissue growth factor. *Genes Dev.* **8**, 1489-1501.

Mason, E. D., Williams, S., Grotendorst, G. R. and Marsh, J. L. (1997). Combinatorial signaling by Twisted Gastrulation and Decapentaplegic. *Mech. Dev.* **64**, 61-75.

Massague, J. and Chen, Y. G. (2000). Controlling TGF-beta signaling. *Genes Dev.* **14**, 627-644.

McMahon, J. A., Takada, S., Zimmerman, L. B., Fan, C. M., Harland, R. M. and McMahon, A. P. (1998). Noggin-mediated antagonism of BMP signaling is required for growth and patterning of the neural tube and somite. *Genes Dev.* **12**, 1438-1452.

Meyers, E. N., Lewandoski, M. and Martin, G. R. (1998). An Fgf8 mutant allelic series generated by Cre- and Flp-mediated recombination. *Nat. Genet.* **18**, 136-141.

Ming, J. E. and Muenke, M. (2002). Multiple hits during early embryonic development: digenic diseases and holoprosencephaly. *Am. J. Hum. Genet.* **71**, 1017-1032.

Miyama, K., Yamada, G., Yamamoto, T. S., Takagi, C., Miyado, K., Sakai, M., Ueno, N. and Sibuya, H. (1999). A BMP-inducible gene, dlx5, regulates osteoblast differentiation and mesoderm induction. *Dev. Biol.* **208**, 123-133.

Muenke, M. and Beachy, P. A. (2000). Genetics of ventral forebrain development and holoprosencephaly. *Curr. Opin. Genet. Dev.* **10**, 262-269.

Nosaka, T., Morita, S., Kitamura, H., Nakajima, H., Shibata, F., Morikawa, Y., Kataoka, Y., Ebihara, Y., Kawashima, T., Itoh, T. et al. (2003). Mammalian twisted gastrulation is essential for skeleto-lymphogenesis. *Mol. Cell Biol.* **23**, 2969-2980.

Oelgeschläger, M., Larrain, J., Geissert, D. and de Robertis, E. M. (2000). The evolutionarily conserved BMP-binding protein Twisted gastrulation promotes BMP signalling. *Nature* **405**, 757-763.

Oelgeschläger, M., Reversade, B., Larrain, J., Little, S., Mullins, M. C. and de Robertis, E. M. (2003a) The pro-BMP activity of Twisted gastrulation is independent of BMP binding. *Development* **130**, 4047-4056.

Oelgeschläger, M., Kuroda, H., Reversade, B. and de Robertis, E. M. (2003b) Chordin is required for the Spemann organizer transplantation phenomenon in Xenopus embryos. *Dev. Cell* **4**, 219-230.

Ohkubo, Y., Chiang, C. and Rubenstein, J. L. (2002). Coordinate regulation and synergistic actions of BMP4, SHH and FGF8 in the rostral prosencephalon regulate morphogenesis of the telencephalic and optic vesicles. *Neuroscience* **111**, 1-17.

Oliver, G., Mailhos, A., Wehr, R., Copeland, N. G., Jenkins, N. A. and Gruss, P. (1995). Six3, a murine homologue of the sine oculis gene, demarcates the most anterior border of the developing neural plate and is expressed during eye development. *Development* **121**, 4045-4055.

Piccolo, S., Agius, E., Lu, B., Goodman, S., Dale, L. and de Robertis, E. M. (1997). Cleavage of Chordin by Xolloid metalloprotease suggests a role for proteolytic processing in the regulation of Spemann organizer activity. *Cell* **91**, 407-416.

Ross, J. J., Shimmi, O., Vilmos, P., Petryk, A., Kim, H., Gaudenz, K., Hermanson, S., Ekker, S. C., O'Connor, M. B. and Marsh, J. L. (2001). Twisted gastrulation is a conserved extracellular BMP antagonist. *Nature* **410**, 479-483.

Rubenstein, J. L., Shimamura, K., Martinez, S. and Puelles, L. (1998). Regionalization of the prosencephalic neural plate. *Annu. Rev. Neurosci.* **21**, 445-477.

Scott, I. C., Blitz, I. L., Pappano, W. N., Imamura, Y., Clark, T. G., Steiglitz, B. M., Thomas, C. L., Maas, S. A., Takahara, K., Cho, K. W. et al. (1999). Mammalian BMP-1/Tolloid-related metalloproteinases, including novel family member mammalian Tolloid-like 2, have differential enzymatic activities and distributions of expression relevant to patterning and skeletogenesis. *Dev. Biol.* **213**, 283-300.

Scott, I. C., Blitz, I. L., Pappano, W. N., Maas, S. A., Cho, K. W. and Greenspan, D. S. (2001). Homologues of Twisted gastrulation are extracellular cofactors in antagonism of BMP signalling. *Nature* **410**, 475-478.

Shimmi, O. and O'Connor, M. B. (2003). Physical properties of Tld, Sog, Tsg and Dpp protein interactions are predicted to help create a sharp boundary in BMP signal during dorsal-ventral patterning of the Drosophila embryo. *Development* **130**, 4673-4682.

Storm, E. E., Rubenstein, J. L. and Martin, G. R. (2003). Dosage of Fgf8 determines whether cell survival is positively regulated in the developing forebrain. *Proc. Natl. Acad. Sci. USA* **100**, 1757-1762.

Stottmann, R. W., Anderson, R. M. and Klingensmith, J. (2001). The BMP antagonists Chordin and Noggin have essential but redundant roles in mouse mandibular outgrowth. *Dev. Biol.* **240**, 457-473.

Sun, X., Meyers, E. N., Lewandoski, M. and Martin, G. R. (1999). Targeted disruption of Fgf8 causes failure of cell migration in the gastrulating mouse embryo. *Genes Dev.* **13**, 1834-1846.

Theiler, K. (1988). Vertebral malformations. *Adv. Anat. Embryol. Cell Biol.* **112**, 1-99.

Thomas, P. Q., Brown, A. and Beddington, R. S. (1998). Hex: a homeobox gene revealing peri-implantation asymmetry in the mouse embryo and an early transient marker of endothelial cell precursors. *Development* **125**, 85-94.

Trumpp, A., Depew, M. J., Rubenstein, J. L., Bishop, J. M. and Martin, G. R. (1999). Cre-mediated gene inactivation demonstrates that FGF8 is required for cell survival and patterning of the first branchial arch. *Genes Dev.* **13**, 3136-3148.

Vilmos, P., Gaudenz, K., Hegedus, Z. and Marsh, J. L. (2001). The Twisted gastrulation family of proteins, together with the IGFBP and CCN families, comprise the TIC superfamily of cysteine rich secreted factors. *Mol. Pathol.* **54**, 317-323.

Wieschaus, E., Nusslein-Volhard, C. and Jurgens, G. (1984). Mutations affecting the pattern of the larval cuticle in *Drosophila melanogaster*. *Wilhelm Roux's Arch. Dev. Biol.* **193**, 296-307.

Winnier, G., Blessing, M., Labosky, P. A. and Hogan, B. L. (1995). Bone morphogenetic protein-4 is required for mesoderm formation and patterning in the mouse. *Genes Dev.* **9**, 2105-2116.

Zhao, M., Harris, S. E., Horn, D., Geng, Z., Nishimura, R., Mundy, G. R. and Chen, D. (2002). Bone morphogenetic protein receptor signaling is necessary for normal murine postnatal bone formation. *J. Cell Biol.* **157**, 1049-1060.